

# ORFEUS-II Observations of the Ultraviolet-Bright Star Barnard 29 in M13<sup>1</sup>

W. Van Dyke Dixon and Mark Hurwitz  
*Space Sciences Laboratory*

*University of California, Berkeley, California 94720-5030*  
vand@ssl.berkeley.edu

To appear in *The Astrophysical Journal (Letters)*

## Abstract

The UV-bright star Barnard 29 in the globular cluster M13 was observed for 5300 seconds with the Berkeley spectrometer on the ORFEUS-SPAS II mission in 1996 November–December. The resulting spectrum extends from the interstellar cutoff at 912 Å to  $\sim 1200$  Å at a resolution of  $\sim 0.33$  Å. It shows numerous absorption features, both photospheric and interstellar, but no significant emission other than diffuse emission of local origin. The Kurucz synthetic stellar spectrum that best fits the data has  $T_{eff} = 21,000$  K,  $\log g = 3.0$ , and  $[M/H] = -2.5$ . This effective temperature and surface gravity are consistent with previous results, but the derived metallicity is lower than that of other M13 giants, for which  $[Fe/H] = -1.60$ . Using high-resolution synthetic spectra, we determine the photospheric abundances of C, S, and Fe, species unobservable in the optical. We find  $\log \epsilon(C) = 6.15 \pm 0.10$ ,  $\log \epsilon(S) = 5.34 \pm 0.50$ , and  $\log \epsilon(Fe) = 5.30_{-0.26}^{+0.22}$ . Again, the Fe abundance is lower than expected. This anomaly may reflect selective condensation of metals onto dust grains at the end of the AGB phase, as has been suggested for some cooler post-AGB stars with peculiar Fe abundances.

*Subject headings:* globular clusters: individual (M 13) — stars: evolution — stars individual (Barnard 29 M 13) — ultraviolet: stars

## 1. INTRODUCTION

The ultraviolet-bright stars in globular clusters lie in the upper left corner of the color-magnitude diagram. Brighter than the horizontal branch (HB)

<sup>1</sup>Based on the development and utilization of ORFEUS (Orbiting and Retrievable Far and Extreme Ultraviolet Spectrometers), a collaboration of the Institute for Astronomy and Astrophysics at the University of Tübingen, the Space Astrophysics Group of the University of California at Berkeley, and the Landessternwarte Heidelberg.

and bluer than the asymptotic giant branch (AGB), this class of objects includes evolved HB, post-HB, and post-AGB stars. Fewer than 50 globular cluster UV-bright stars are known; of these, only 13–16 may be classified as post-AGB stars (de Boer 1987). The brief post-AGB phase (typically  $10^4$  years; Schönberner 1981, 1983) is one of the least well understood phases of stellar evolution, yet the nucleosynthesis, dredge-up, and mass-loss processes that occur during this phase are principally responsible for the enrichment of the interstellar medium (ISM), and for carbon and oxygen in particular (Wheeler, Sneden, & Truran 1989). To improve our understanding of the final stages of a star’s lifetime, as well as the mechanisms by which it enriches the ISM, we observed the UV-bright star Barnard 29 with the Berkeley spectrograph on the ORFEUS-SPAS II mission.

Barnard 29 is a well-studied UV-bright star in the globular cluster M13 (Strom & Strom 1970; de Boer 1985; Conlon, Dufton, & Keenan 1994). Stellar and cluster parameters are presented in Table 1. Recently, Conlon et al. (1994) used an LTE analysis of high-resolution optical spectra of Barnard 29 to derive its atmospheric parameters and abundances. The authors found  $T_{eff} = 20,000$  K and  $\log g = 3.0$ , confirming Barnard 29 as a post-AGB star. The star’s helium abundance is nearly solar. Metal abundances are about 1 dex below solar, except for carbon, which is deficient by some 2.4 dex, and nitrogen, which shows a much smaller underabundance of 0.7 dex (relative to solar). The authors were able to set only upper limits on the abundance of three important elements, C, S, and Fe. We use the far-UV spectrum of Barnard 29 to set independent constraints on the star’s atmospheric parameters and to determine these elemental abundances.

## 2. OBSERVATIONS AND DATA REDUCTION

The Berkeley spectrograph, located at the prime focus of the 1-m ORFEUS telescope, flew aboard the space shuttle *Columbia* on the ORFEUS-SPAS II mission in 1996 November–December. The spectrograph’s far-UV sensitivity extends from the interstellar cutoff at 912 Å to about 1220 Å, with a mean spectral resolution of  $95 \text{ km s}^{-1}$  FWHM (about 0.33 Å) for point sources. Its effective area peaks at about  $9 \text{ cm}^2$  near 1000 Å. The general design of the Berkeley spectrograph is discussed by Hurwitz & Bowyer

Table 1: Stellar Parameters

Parameter	Value	Reference
Spectral Type	B2p	1
$V$	13.14	2
$B - V$	-0.16	2
$E(B - V)$	0.02	3
Distance (kpc)	7.2	3
$\log N_{\text{H}}$ ( $\text{cm}^{-2}$ )	20.17	4
$V_{r,\text{cluster}}$ ( $\text{km s}^{-1}$ )	$-241 \pm 10$	5
$V_{r,\text{star}}$ ( $\text{km s}^{-1}$ )	$-251 \pm 7$	6
$[\text{Fe}/\text{H}]_{\text{cluster}}$	-1.60	7
$T_{\text{eff}}$ (K)	$20,000 \pm 1000$	6
$\log g$ (dex)	$3.0 \pm 0.1$	6

REFERENCES: (1) Garrison & Albert 1986; (2) Cudworth & Monet 1979; (3) Djorgovski 1993; (4) Stark et al. 1992; (5) Arp 1965; (6) Conlon et al. 1994; (7) Kraft et al. 1997.

(1986, 1996), while its calibration and performance on the ORFEUS-SPAS II mission are described by Hurwitz et al. (1998).

Two successful pointings at Barnard 29 were obtained during the flight, totaling 5300 s. The resulting spectra were each rebinned to a common set of 0.165 Å wavelength bins (about half the instrumental resolution), then background subtracted, scaled to correct for detector dead-time effects, and wavelength and flux calibrated as described in Hurwitz et al. (1998). The flux calibration is based on in-flight observations of the hot DA white dwarf HZ43 and is believed accurate to about 10%. The spectra were weighted by their integration times and averaged to produce the final calibrated spectrum presented in Fig. 1.

### 3. ANALYSIS

#### 3.1. Atmospheric Parameters

We begin by deriving an independent set of stellar atmospheric parameters. To this end, we combine our data with an *IUE* spectrum of Barnard 29 to produce a complete stellar spectrum extending from  $\sim 2000$  Å to the Lyman limit and fit it with the synthetic stellar spectra of Kurucz (1992). The Kurucz stellar atmosphere models incorporate statistically correct line strengths for some sixty million atomic and molecular transitions and are available for scaled solar abundances<sup>2</sup> [M/H] between +1.0 and -5.0 (where M represents all elements heavier than helium). The models provide a thorough treatment of line blanketing by metals, but their assumption of local thermodynamic equilibrium (LTE) neglects the non-LTE processes which may be important for hot, low-gravity stars.

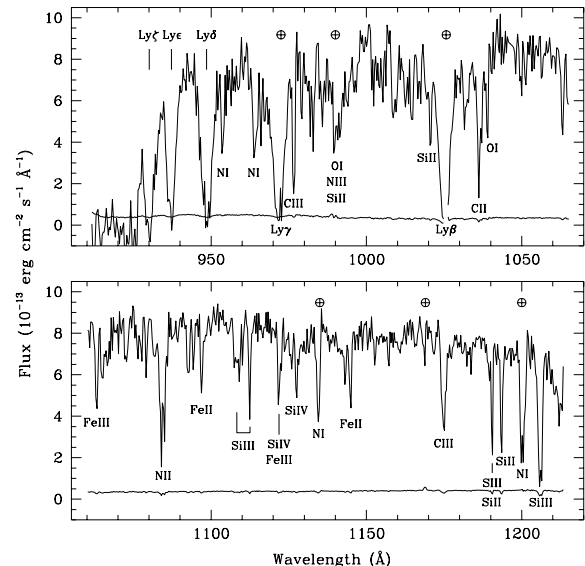


Fig. 1.— Far-UV spectrum of the UV-bright star Barnard 29 in M13 obtained with the Berkeley spectrometer on the ORFEUS telescope. The data are flux-calibrated, airglow-subtracted, and binned (for this figure only) by 0.33 Å. No reddening correction has been applied. The error spectrum is overplotted, and principal absorption lines (mostly interstellar) are identified. Residual airglow features are marked with ⊕.

dances<sup>2</sup> [M/H] between +1.0 and -5.0 (where M represents all elements heavier than helium). The models provide a thorough treatment of line blanketing by metals, but their assumption of local thermodynamic equilibrium (LTE) neglects the non-LTE processes which may be important for hot, low-gravity stars.

Following Conlon et al. (1994), we obtained seven *IUE* low-resolution spectra of Barnard 29 (SWP 8778, 8779, 9300, 9578, 9600, 11159, and 31824) from the National Space Science Data Center and averaged them, weighting by the individual exposure times. The *IUE* and ORFEUS spectra were then binned by 10 Å to match the resolution of the Kurucz models. Error bars for each ORFEUS data point were set to 3% of the total observed flux (spectrum +

<sup>2</sup>We adopt the usual spectroscopic notations in this paper, namely  $[X] \equiv \log_{10}(X)_{\text{star}} - \log_{10}(X)_{\odot}$  for any quantity  $X$ , and  $\log \epsilon(X) \equiv \log(N_X/N_{\text{H}}) + 12.0$  for absolute number density abundances.

background) to account for fluctuations in the detector response on large spatial scales (Hurwitz et al. 1998). For consistency, error bars for the *IUE* data were set in the same way. The combined spectra were fit with Kurucz (1992) model spectra using the non-linear curve-fitting program SPECFIT (Kriss 1994) to perform a  $\chi^2$  minimization. Within SPECFIT, models are interpolated to the exact wavelength of each data point, reddened with a Cardelli, Clayton, & Mathis (1989) extinction curve assuming  $E(B-V) = 0.02$  and  $R_V = 3.1$ , and scaled by a transmission function to account for interstellar H I and O I along the line of sight, derived from the Bell Labs 21 cm survey (Stark et al. 1992) according to the prescription of Hurwitz, Jelinsky, & Dixon (1997). Free parameters in the fit are the normalization and wavelength offset of the model spectrum.

The Kurucz model which best fits the data has  $T_{eff} = 21,000$  K,  $\log g = 3.0$ , and  $[M/H] = -2.5$ . The combined spectrum and best-fitting model are plotted in Fig. 2. We see that the model somewhat underpredicts the flux between Lyman  $\beta$  and Lyman  $\alpha$ . Whether this discrepancy is due to abundance anomalies or non-LTE effects must await further analysis. (For a more complete discussion of the limitations of this technique, see Dixon, Davidsen, & Ferguson 1994, 1995.) From the distribution of  $\chi^2$  among the various Kurucz models, we estimate that the uncertainty in the best-fit parameters is approximately 1000 K in  $T_{eff}$ , 0.25 dex in  $\log g$ , and 0.5 dex in  $[M/H]$ , though we note that there are no Kurucz models with  $\log g < 3.0$  at the best-fit temperature. These values of effective temperature and surface gravity are consistent with those derived by Conlon et al. (1994) from *IUE* data alone and from absorption-line fits to the optical spectrum. The metallicity of the best-fit Kurucz model is, however, considerably less than that of the cluster, for which  $[Fe/H] = -1.60$  (Kraft et al. 1997).

To constrain the photospheric abundances of Barnard 29, we consider only the ORFEUS spectrum, binned to  $0.165 \text{ \AA}$ . We generate high-resolution synthetic stellar spectra using the stellar atmospheres of Kurucz (1992) and the synthetic spectral codes of Hubeny (1988). In producing these models, we have made extensive use of the techniques and results of Brown, Ferguson, & Davidsen (1996), which should be consulted for details of our method.

Adopting the stellar atmospheric parameters and abundances derived by Conlon et al. (1994), we begin

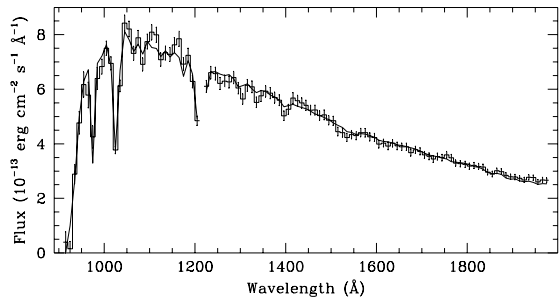


Fig. 2.— Combined ORFEUS ( $\lambda < 1190 \text{ \AA}$ ) and *IUE* spectra of Barnard 29. The data have been binned by  $10 \text{ \AA}$  and are shown as a histogram. Overplotted is the best-fitting Kurucz (1992) model, with  $[M/H] = -2.0$ ,  $T_{eff} = 21,000$  K, and  $\log g = 3.0$ . The model has been reddened with a Cardelli et al. (1989) extinction curve assuming  $E(B-V) = 0.02$  and  $R_V = 3.1$  and includes absorption due to atomic hydrogen and oxygen assuming a column density of  $\log N(\text{H I}) = 20.26$ .

with a single stellar model atmosphere (am15t20000-g30k2.dat; Kurucz 1992) and adjust only the abundances of elements included in the synthetic spectrum calculation. We use SPECFIT to compare a series of models, identical save for the abundance of the species in question, to the region about a particular line. Given a grid of such models, SPECFIT interpolates among them to determine the best-fit abundance, then sets a  $1-\sigma$  error bar on the result. The error bar reflects uncertainties both in the continuum placement and the strength of any nearby lines.

We have determined abundances for all of the elements measured by Conlon et al. (He, N, O, Al, Si) except Mg, for which our model predicts no significant absorption in the far UV. In all cases, our results are consistent with the optically-determined values, though our error bars are usually larger, reflecting the lower resolution of our data. We will not present those results here. Instead, we discuss the three species not available in the optical, C, S, and Fe.

### 3.2. Abundances

#### 3.2.1. Carbon

The two strongest carbon lines in the far UV are C III  $\lambda 977$  and C III  $\lambda 1176$ . Brown et al. (1996) find that the C III  $\lambda 1176$  feature is useful for estimating

the carbon abundance, as its strength is relatively insensitive to changes in temperature and gravity. The lines are due to an excited-state transition and thus uncontaminated by interstellar absorption. Using this feature, we have determined the star’s carbon abundance to be  $6.15 \pm 0.10$  dex [Fig. 3(a)].

### 3.2.2. Sulfur

Our models predict far-UV absorption from three ionization states of sulfur, S II, S III, and S IV. We have found, however, that most of the S II lines yield abundances far lower than do the S III and S IV lines. This would suggest that the model’s effective temperature is too low, but raising  $T_{eff}$  by 1000 K, the most allowed by the optical and far-UV fits, does not relieve the discrepancy, which may instead reflect non-LTE effects not included in our model atmosphere. We thus use only the high-ionization lines to constrain the sulfur abundance. The five strongest S III and S IV lines in our bandpass and the abundances or limits derived from each are S IV  $\lambda 1062.7$ ,  $< 0.95$ ; S IV  $\lambda\lambda 1073.0, 1073.5$ ,  $5.33 \pm 0.77$ ; S III  $\lambda 1077.1$ ,  $6.99 \pm 1.52$ ; S III  $\lambda\lambda 1143.6, 1143.9$ ,  $5.41 \pm 0.79$ ; and S III  $\lambda 1190.2$ ,  $2.04 \pm 2.02$ . The scatter in these results is due, in part, to line blending with nearby features (e.g., Cr III  $\lambda 1062.7$ , Fe III  $\lambda 1143.7$ , and Si II  $\lambda 1190.4$ ) and poor fits to the local stellar continuum. Ignoring the upper limit, we find a weighted mean of  $\log \epsilon(S) = 5.34 \pm 0.50$ . Figure 3(b) shows the region 1057–1083 Å overplotted by a synthetic spectrum with our mean sulfur abundance.

### 3.2.3. Iron

A number of strong iron lines are predicted by our models. Unfortunately, they either lie in regions where the continuum is poorly fit or are contaminated by strong interstellar absorption. Instead of fitting individual features, we have thus chosen to fit a band of iron lines and the nearby continuum in a well-behaved region of the spectrum.

Figure 3(c) shows the spectrum of Barnard 29 between 1115 and 1160 Å. (The strong interstellar and airglow features of N I  $\lambda 1134$  are excluded from the fit.) The iron spectrum, showing the band between 1120 and 1132 Å, is plotted at the top of the figure. The model includes a synthetic ISM spectrum (also shown) composed of Fe II, Fe III, and P II lines; these features are modeled assuming a Doppler parameter  $b = 10$  km s $^{-1}$ . In the fit, the column density of each

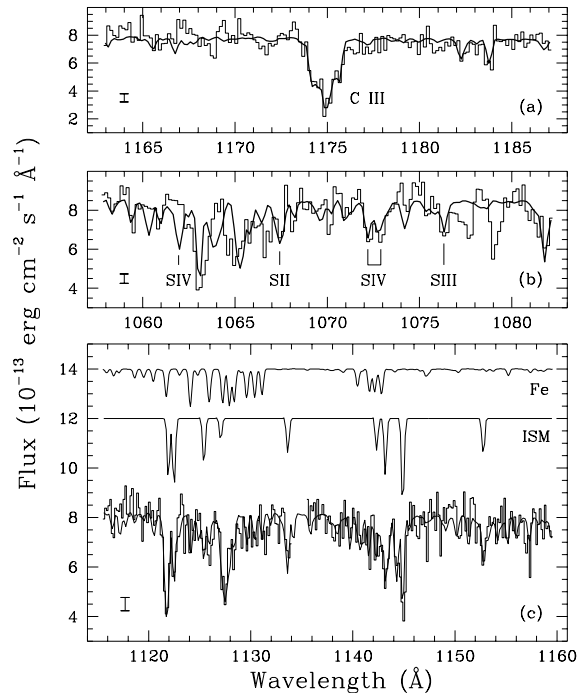


Fig. 3.— (a) The spectrum of Barnard 29 in the region of C III  $\lambda 1176$  is plotted as a histogram. The smooth curve represents our best-fitting model, with a carbon abundance of 6.15. The mean  $1-\sigma$  uncertainty in this region is indicated at lower left. (b) Sulfur features in the spectrum of Barnard 29. A model with the adopted sulfur abundance of 5.34 is overplotted. (c) Fitting the iron abundance of Barnard 29. *Top curve:* The ratio of a synthetic stellar spectrum with best-fitting iron abundance  $\log \epsilon(\text{Fe}) = 5.30$  to one with no iron lines, reflecting the absorption due to iron (mostly Fe III) in the photosphere. *Middle curve:* ISM features (due to Fe II, Fe III, and P II) included in the model fit. The ISM and iron spectra are normalized to the stellar continuum level, then offset in flux space for clarity. *Bottom curve:* Histogram is the observed spectrum; smooth line is the best-fitting model.

IS species is allowed to vary independently. Synthetic spectra with our best-fit sulfur abundance exhibit a S II  $\lambda 1124$  feature considerably stronger than is present in the data, so we have set the sulfur abundance to zero in these models. Because the final model contains so many independent components, we set error bars on the iron abundance by hand, raising and lowering  $\log \epsilon(\text{Fe})$  from the best-fit level until  $\Delta\chi^2 = 1$  (corresponding to a  $1\text{-}\sigma$  deviation for a single interesting parameter; Avni 1976). We find  $\log \epsilon(\text{Fe}) = 5.30^{+0.22}_{-0.26}$ . The best-fit model is overplotted.

The best-fit iron abundance is more than 0.5 dex below that of the Kurucz atmosphere model from which we derive our synthetic spectra. To check whether this discrepancy has a significant effect on our result, we generate a set of three synthetic spectra, with  $\log \epsilon(\text{Fe}) = 5.0, 5.5,$  and  $6.0$ , based on Kurucz model atmospheres with  $[\text{M}/\text{H}] = -2.5, -2.0,$  and  $-1.5$ , respectively. The models are otherwise the same as before. Allowing SPECFIT to interpolate among them, we find that the best-fit abundance is  $\log \epsilon(\text{Fe}) = 5.28^{+0.26}_{-0.19}$ , consistent with our previous result. We conclude that a small discrepancy in the metallicity of the input stellar atmosphere model is not a significant source of error in our derived abundances.

#### 4. DISCUSSION

The CNO abundance pattern seen in Barnard 29 is observed in a number of red giants in M13, four carbon-poor planetary nebulae, and all of the high-latitude B-type post-AGB candidates (Conlon et al. 1994). According to current stellar evolutionary theory, such abundance ratios are expected of stars that leave the AGB before third dredge up brings significant nuclear-processed material to the surface (Iben & Renzini 1983). We would therefore expect Barnard 29 to have an iron abundance similar to other M13 giants, for which  $[\text{Fe}/\text{H}] = -1.60$  (Kraft et al. 1997). Instead, we find that the star has an iron abundance 2 dex or more below solar. Low metallicities are seen in other UV-bright stars in globular clusters, but not all: for vZ 1128 in M3,  $[\text{M}/\text{H}] = -3.5 \pm 1.5$ , nearly 2 dex below the cluster mean, while BS in 47 Tuc and UV5 in NGC 1851 have metallicities consistent with the cluster mean (Dixon et al. 1994, 1995).

For BD+33°2642, a planetary nebula central star in the galactic halo, Napiwotzki, Heber, & Köppen (1994) derive an abundance distribution similar to

that of Barnard 29: He is near solar, C, N, O, Mg, Si are depleted by about 1 dex, and Fe is depleted by 2 dex relative to the sun. The authors suggest that the low Fe abundance may be the result of gas-dust fractionation, a process proposed to explain the chemical peculiarities in some cooler post-AGB stars. In this scenario, metals with a high condensation temperature condense into dust grains and are removed by radiation pressure, while elements with lower condensation temperatures remain. Most models require a binary system to support a circumstellar disk about the AGB star (for a review, see Trams, Waelkens, & Waters 1993), but a single-star model has been proposed by Mathis & Lamers (1992). One of its predictions, however, is that  $N(\text{C}) \approx N(\text{O})$  in the resulting iron-poor photosphere, a condition not seen in Barnard 29.

The abundances presented here are derived under the assumption of LTE. Because Barnard 29 is a low-gravity star, non-LTE effects may be significant. The strength of such effects and their influence on the derived stellar abundances are difficult to determine *a priori*. Future work will address these issues using appropriate non-LTE model atmospheres.

This research has made use of the NASA ADS Abstract Service and the Catalogue Service of the CDS, Strasbourg, France. We thank R. Kurucz for providing a computer-readable tape of his stellar atmosphere models. We thank I. Hubeny for providing his spectral synthesis codes and T. Brown for assistance in using them. We acknowledge our colleagues on the ORFEUS team and the many NASA and DARA personnel who helped make the ORFEUS mission successful. This work is supported by NASA grant NAG5-696.

## REFERENCES

- Arp, H. C. 1965, in *Galactic Structure*, ed. A. Blaauw & M. Schmidt (Chicago: Univ. Chicago Press), 401
- Avni, Y. 1976, *ApJ*, 210, 642
- Brown, T. M., Ferguson, H. C., & Davidsen, A. F. 1996, *ApJ*, 472, 327
- Cardelli, J. A., Clayton, G. C., & Mathis, J. S. 1989, *ApJ*, 345, 245 (CCM)
- Conlon, E. S., Dufton, P. L., & Keenan, F. P. 1994, *A&A*, 290, 897
- Cudworth, K. M., & Monet, D. G. 1979, *AJ*, 84, 774
- de Boer, K. S. 1985, *A&A*, 142, 321
- de Boer, K. S. 1987, in *IAU Colloq. 95, The Second Conference on Faint Blue Stars*, ed. A. G. D. Phillip, D. Hayes, & J. Leibert (Schenectady: L. Davis Press), 95
- Dixon, W. V., Davidsen, A. F., & Ferguson, H. C. 1994, *AJ*, 107, 1388
- Dixon, W. V., Davidsen, A. F., & Ferguson, H. C. 1995, *ApJ*, 454, L47
- Djorgovski, S. 1993, in *ASP Conf. Ser. 50, Structure and Dynamics of Globular Clusters*, ed. S. Djorgovski & G. Meylan (San Francisco: ASP), 373
- Garrison, R. F., & Albert, C. E. 1986, *ApJ*, 300, L69
- Hubeny, I. 1988, *Comput. Phys. Comm.*, 52, 103
- Hurwitz, M., et al. 1998, *ApJ*, this issue
- Hurwitz, M., & Bowyer, S. 1986, *Proceedings of SPIE*, 627, 375
- Hurwitz, M., & Bowyer, S. 1996, in *Astrophysics in the Extreme Ultraviolet*, ed. S. Bowyer & R. F. Malina (Dordrecht: Kluwer), 601
- Hurwitz, M., Jelinsky, P., & Dixon, W. V. 1997, *ApJ*, 481, L31
- Iben, I., Jr., & Renzini, A. 1983, *ARA&A*, 21, 271
- Kraft, R. P., Sneden, C., Smith, G. H., Shetrone, M. D., Langer, G. E., & Pilachowski, C. A. 1997, *AJ*, 113, 279
- Kriss, G. A. 1994, in *ASP Conf. Ser. 61, Astronomical Data Analysis Software and Systems III*, ed. D. R. Crabtree, R. J. Hanisch, & J. Barnes (San Francisco: ASP), 437
- Kurucz, R. L. 1992, in *IAU Symposium No. 149, The Stellar Populations of Galaxies*, ed. B. Barbuy & A. Renzini (Dordrecht: Kluwer), 225
- Mathis, J. S., & Lamers, H. J. G. L. M. 1992, *A&A*, 259, L39
- Napiwotzki, R., Heber, U., & Köppen, J. 1994, *A&A*, 292, 239
- Schönberner, D. 1981, *A&A*, 103, 119
- Schönberner, D. 1983, *ApJ*, 272, 708
- Stark, A. A., Gammie, C. F., Wilson, R. W., Bally, J., Linke, R. A., Heiles, C., & Hurwitz, M. 1992, *ApJS*, 79, 77
- Strom, S. E., & Strom, K. M. 1970, *ApJ*, 159, 195
- Trams, N. R., Waelkens, C., & Waters, L. B. F. M. 1993, in *ASP Conf. Ser. 45, Luminous High-Latitude Stars*, ed. D. D. Sasselov (San Francisco: ASP), 103
- Wheeler, J. C., Sneden, C., & Truran, J. W. 1989, *ARA&A*, 27, 279